

Contents lists available at ScienceDirect

Physics Letters B

www.elsevier.com/locate/physletb

Scattering amplitudes with off-shell quarks

A. van Hameren^{a,*}, K. Kutak^a, T. Salwa^{a,b}^a The H. Niewodniczański Institute of Nuclear Physics, Polish Academy of Sciences, Radzikowskiego 152, 31-342 Cracow, Poland^b Faculty of Physics, Astronomy and Applied Computer Science, Jagiellonian University, Reymonta 4, 30-059 Cracow, Poland

ARTICLE INFO

Article history:

Received 20 August 2013

Received in revised form 1 October 2013

Accepted 16 October 2013

Available online 24 October 2013

Editor: B. Grinstein

ABSTRACT

We present a prescription to calculate manifestly gauge invariant tree-level scattering amplitudes for arbitrary scattering processes with off-shell initial-state quarks within the kinematics of high-energy scattering.

© 2013 Elsevier B.V. All rights reserved.

1. Introduction

Factorization procedures are the key to the application of perturbative QCD to the calculation of cross sections of hard scattering processes at the Large Hadron Collider. They follow the physical picture of the parton model, in which it is eventually the quarks and gluons, or *partons*, inside the colliding hadrons that interact in the hard scattering process. In *collinear factorization*, these partons simply transport a fraction of the momentum of the hadron into the scattering process, encoded by a single proportionality factor usually denoted by x . The factorization happens via the convolution of a process-dependent partonic cross section with universal parton density functions (pdfs), which only depend on this x variable and an unphysical scale, the factorization scale. The total cross section is independent of this scale if all orders in perturbation theory are taken into account, and in [1] it has been proven that this indeed works and that the procedure is consistent.

One may then wonder whether it is possible to generalize the factorization procedure, and allow for the partons to carry momentum components into the partonic scattering process that are independent of the original hadron momentum, or more specifically, that are transverse. This would allow for calculations at leading order in QCD to incorporate kinematical effects that only appear at higher orders within collinear factorization.

The extension of collinear factorization to allow for inclusion transverse momentum effects goes under a name *Transversal Momentum Dependent* (TMD) factorization (we refer the reader to [2] and references therein) and is in principle valid at large x . It has been realized in [3,4] that the introduction of the extra momentum components implies an extra energy scale which may be assumed to be much lower than the total energy of hadronic scattering process. This approach goes under the name of *high-energy factor-*

ization. It becomes relevant when the transverse components are sizable compared to the longitudinal components carried into the partonic process, *i.e.* for low values of x .

The partonic cross section within high-energy factorization requires matrix elements with off-shell initial-state partons and needs to be convoluted with parton densities which depend on longitudinal and transverse momentum [5–16]. Various approaches to calculate the matrix elements for off-shell initial-state gluons exist [17–20]. The main issue is to ensure that they are gauge invariant and that they satisfy the necessary Ward identities. While far less popular in literature, approaches for off-shell quarks have also been developed. In particular, the effective action approach for off-shell gluons [17] has also been applied for off-shell quarks [21], and this approach has been followed *e.g.* in [22]. Recently, it has been used to calculate scattering amplitudes for several scattering processes in [23]. Other recent work involving off-shell quarks can be found in [24–28].

In this Letter, we will derive a prescription to calculate manifestly gauge invariant tree-level scattering amplitudes with off-shell initial-state quarks and an arbitrary number of final-state particles. It is essentially the generalization of the work in [20] for quarks, and can straightforwardly be implemented in numerical programs using the well-known efficient methods for tree-level calculations. Whereas prescription in [20] for gluons was shown to be equivalent to the effective action approach of [17], the prescription for quarks presented here will be shown to be equivalent to the effective action approach of [21].

2. Construction

In [20], a pair of auxiliary quarks was introduced enabling the embedding of the process $g^*g^* \rightarrow X$ with the off-shell gluons into the process $q_Aq_B \rightarrow q_Aq_B X$ with on-shell quarks, and where X represents any set of final-state particles. It was shown that by applying eikonal Feynman rules to the quark lines, gauge invariant

* Corresponding author.

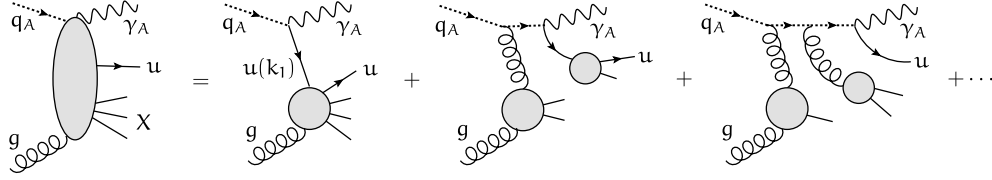


Fig. 1. A few terms in the classification of the graphs contributing to $q_A g \rightarrow \gamma_A u X$ w.r.t. the gluons attached to the quark line.

scattering amplitudes are obtained that are defined in the desired kinematical configuration that is relevant in high-energy factorization. This configuration is such, that the off-shell initial-state partons carry momenta

$$k_1^\mu = x_1 \ell_1^\mu + k_{1\perp}^\mu, \quad k_2^\mu = x_2 \ell_2^\mu + k_{2\perp}^\mu, \quad (1)$$

where ℓ_1, ℓ_2 are the light-like momenta associated with the colliding hadrons, and where $k_{1\perp}, k_{2\perp}$ are transverse to both ℓ_1 and ℓ_2 . The momentum fractions x_1, x_2 are between 0 and 1.

It was stressed in [20] that the formalism works for two off-shell gluons, but it was also clear that the treatment of the gluons is completely independent, and that the formalism can be viewed as a trivial generalization from one off-shell gluon to two off-shell gluons. Here, we will consider the case of a single off-shell initial-state quark, and it will be clear that the situation can be trivially generalized to the case of two off-shell initial-state partons, be it quarks and/or gluons. So we consider the process

$$u^* g \rightarrow u X, \quad (2)$$

where X represents an arbitrary, but definite, set of final-state particles. We will follow the strategy of embedding this process into a larger on-shell process again. To this end, we introduce an auxiliary quark q_A and an auxiliary photon γ_A which interact with the u -quark via the vertex

$$q_A \dots \gamma_A \dots u = -i \gamma^\mu. \quad (3)$$

The auxiliary photon does not interact with any other particles, and can be interpreted as allowing for neutral flavor-changing currents involving q_A - and u -quarks. It is a color singlet, whereas the quark is in the fundamental representation. The quark further only interacts with gluons via normal quark–gluon vertices. Now, we consider the process

$$q_A g \rightarrow \gamma_A u X. \quad (4)$$

Fig. 1 shows a classification of graphs contributing to the process. The first term on the r.h.s. contains all the graphs with the off-shell quark with momentum k_1 . To arrive at a gauge invariant amplitude, also the other terms have to be taken into account. The momenta of the auxiliary quark q_A and photon γ_A are p_A and $p_{A'}$ respectively, and following the approach of [20], we assign the values

$$p_A^\mu = (\Lambda + x_1) \ell_1^\mu - \frac{k_{1\perp} \cdot \ell_4}{\ell_1 \cdot \ell_2} \ell_3^\mu, \quad p_{A'}^\mu = \Lambda \ell_1^\mu + \frac{k_{1\perp} \cdot \ell_3}{\ell_1 \cdot \ell_2} \ell_4^\mu, \quad (5)$$

where ℓ_3, ℓ_4 span the transverse space, and are defined by

$$\ell_3^\mu = \frac{1}{2} \langle \ell_2 | \gamma^\mu | \ell_1 \rangle, \quad \ell_4^\mu = \frac{1}{2} \langle \ell_1 | \gamma^\mu | \ell_2 \rangle. \quad (6)$$

The momenta in Eq. (5) are on-shell and satisfy

$$p_A^\mu - p_{A'}^\mu = k_1^\mu = x_1 \ell_1^\mu + k_{1\perp}^\mu, \quad (7)$$

as required, for any value of the dimensionless parameter Λ . It was argued in [20] that one can directly assign the spinor $|\ell_1\rangle$ to the auxiliary quark without spoiling gauge invariance:

$$q_A \leftarrow |\ell_1\rangle. \quad (8)$$

We will do the same here, but with assumption that the helicity of the final-state u -quark is negative, so for

$$u\text{-quark} \leftarrow \langle p_u |. \quad (9)$$

where p_u is the momentum of the u -quark. We will come back to the case of positive helicity for the u -quark later. For the polarization vector of γ_A we use the proper normalization of the vector ℓ_4 :

$$\varepsilon_{A'}^\mu = \frac{\sqrt{2}}{[\ell_1 | \ell_2]} \ell_4^\mu. \quad (10)$$

It is a polarization vector for a photon with momentum ℓ_1 and auxiliary vector ℓ_2 , and is also valid for momentum $p_{A'}$ since $p_{A'} \cdot \varepsilon_{A'} = 0$.

On-shellness of all particles involved in the constructed amplitude ensures its gauge invariance. It, however, depends on unphysical imaginary momentum components, and the physical amplitude is extracted by taking the limit of $\Lambda \rightarrow \infty$. This limit only affects the q_A -propagators. For a q_A -line with momentum p we have

$$\frac{i \not{p}}{p^2} \xrightarrow{\Lambda \rightarrow \infty} \frac{i \not{\ell}_1}{2 \ell_1 \cdot p}. \quad (11)$$

The obtained amplitude still needs to be matched to the collinear limit when $k_1^2 \rightarrow 0$. It has to be multiplied by a kinematical factor, which we will now derive. Firstly, the first set of graphs on the r.h.s. of Fig. 1 dominate, since only they contain k_1^2 in the denominator. Let us abbreviate this set by

$$\mathcal{A} = [\Psi | \frac{i k_1}{k_1^2} (-i \not{\varepsilon}_{A'}) | \ell_1] = \frac{1}{k_1^2} [\Psi | k_1 \not{\varepsilon}_{A'} | \ell_1], \quad (12)$$

where $[\Psi |$ represents the blob, excluding the propagator with momentum k_1 . Inserting Eq. (10), we get

$$\mathcal{A} = \frac{1}{k_1^2} [\Psi | k_1 | \ell_1] [\ell_2 | \ell_1] \frac{\sqrt{2}}{[\ell_1 | \ell_2]} = -\frac{\sqrt{2}}{k_1^2} [\Psi | k_1 | \ell_1], \quad (13)$$

and inserting the expansion of k_1 in terms of ℓ_1, ℓ_3, ℓ_4 , we find

$$\mathcal{A} = \frac{\sqrt{2}}{k_1^2} [\Psi | \ell_1] \langle \ell_2 | \ell_1 \rangle \frac{k_{1\perp} \cdot \ell_4}{\ell_1 \cdot \ell_2}. \quad (14)$$

Here, $[\Psi | \ell_1]$ is the amplitude in the collinear limit, modulo a factor $\sqrt{x_1}$. In the collinear case, the on-shell initial-state quark would get a spinor $|x_1 \ell_1] = \sqrt{x_1} |\ell_1]$. Now we note that, for real ℓ_1, ℓ_2 , the vectors ℓ_3 and ℓ_4 are each others complex conjugate, so that

$$k_1^2 = k_{1\perp}^2 = -2 \frac{|k_{1\perp} \cdot \ell_4|^2}{\ell_1 \cdot \ell_2} \quad (15)$$

and, using also $|\langle \ell_2 | \ell_1 \rangle|^2 = 2 \ell_1 \cdot \ell_2$, we find

$$|\mathcal{A}|^2 = -2 \frac{|\Psi | \ell_1 |]^2}{k_1^2} = \frac{|\Psi | x_1 \ell_1 |]^2}{-x_1 k_1^2 / 2}. \quad (16)$$

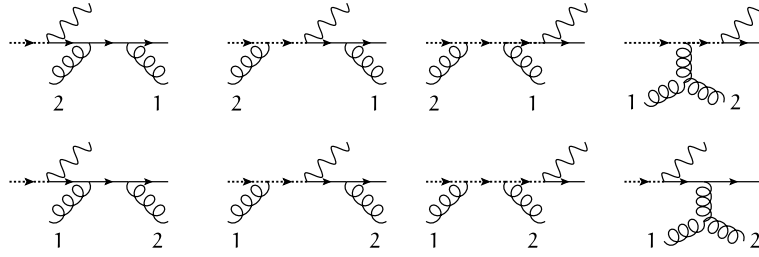


Fig. 2. Graphs contributing to the process $u^*g \rightarrow ug$.

So we conclude that in order to arrive at an amplitude leading to the correct collinear limit, it has to be multiplied with $\sqrt{-x_1 k_1^2/2}$.

The derivation above was for a negative helicity final-state u -quark. For positive helicity, we need to switch the roles of ℓ_3 and ℓ_4 , and assign $q_A \leftarrow |\ell_1\rangle$. The auxiliary photon gets polarization vector $\sqrt{2}\ell_3^\mu/\langle\ell_2|\ell_1\rangle$. For processes with an off-shell initial-state anti-quark, the derivation works quite analogously, with spinors $\langle\ell_1|, [\ell_1]$ for the auxiliary quark. The kinematical factor the amplitude has to be multiplied with is the same for all cases.

We summarize the prescription to calculate gauge invariant tree-level scattering amplitudes with an off-shell initial-state, say u^- , quark that gives the correct collinear limit:

Prescription.

1. Consider the embedding of the process, in which the off-shell u -quark is replaced by an auxiliary quark q_A , and an auxiliary photon γ_A is added in final state.
2. The momentum flow is as if q_A carries momentum k_1 and the momentum of γ_A is identical to 0.
3. γ_A only interacts via Eq. (3), and q_A further only interacts with gluons via normal quark–gluon vertices.
4. q_A -line propagators are interpreted as $i\not{\ell}_1/(2\ell_1 \cdot p)$, and are diagonal in color space.
5. Sum the squared amplitude over helicities of the auxiliary photon. For one helicity, simultaneously assign to the external q_A -quark and to γ_A the spinor and polarization vector

$$|\ell_1], \quad \frac{\langle\ell_1|\gamma^\mu|\ell_2\rangle}{\sqrt{2}[\ell_1|\ell_2]}, \quad (17)$$

and for the other helicity assign

$$|\ell_1], \quad \frac{\langle\ell_2|\gamma^\mu|\ell_1\rangle}{\sqrt{2}\langle\ell_2|\ell_1\rangle}. \quad (18)$$

6. Multiply the amplitude with $\sqrt{-x_1 k_1^2/2}$.

For the rest, normal Feynman rules apply.

Some remarks are at order. Regarding the momentum flow, we stress, as in [20], that momentum components proportional to k_1 do not contribute in the eikonal propagators, and there is a freedom in the choice of the momenta flowing through q_A -lines.

Regarding the sum over helicities, one might argue that only one of them leads to a non-zero result for given helicity of the final-state quark, but there may, for example, be several identical such quarks in the final state with different helicities.

In case of more than one quark in the final state with the same flavor as the off-shell quark, the rules as such admit graphs with γ_A -propagators. These must be omitted. They do not survive the limit $\Lambda \rightarrow \infty$ in the derivation, since the γ_A -propagators are suppressed by $1/\Lambda$.

The rules regarding the q_A -line could be elaborated further like in [20], leading to simplified vertices for gluons attached to this line and reducing the numerator of the eikonal propagators to 1. Formulated as above, however, the prescription is more straightforward and closer to familiar Feynman rules. The equivalent rules for off-shell gluons were presented in [29].

For off-shell initial-state anti-quarks, the spinors and polarization vectors for the auxiliary particles become

$$[\ell_1|, \quad \frac{\langle\ell_1|\gamma^\mu|\ell_2\rangle}{\sqrt{2}[\ell_1|\ell_2]} \quad \text{and} \quad \langle\ell_1|, \quad \frac{\langle\ell_2|\gamma^\mu|\ell_1\rangle}{\sqrt{2}\langle\ell_2|\ell_1\rangle}. \quad (19)$$

The eikonal propagator for the anti-quark carries an extra minus-sign.

Amplitudes with a second off-shell initial-state quark can be constructed introducing a second auxiliary quark q_B and a second auxiliary photon γ_B . This photon does not interact with the q_A -quark, and γ_A does not interact with q_B . The Feynman rules for these auxiliary particles are the same as before, but with the role of ℓ_1 and ℓ_2 interchanged. Amplitudes with an off-shell initial-state quark and an off-shell initial-state gluon can be constructed using the rules presented in [29] for the off-shell gluon.

3. Results

In Appendix A we reproduce some non-trivial expressions for scattering amplitudes with off-shell quarks given earlier in [23], thereby indicating the equivalence of our approach to the effective action approach of [21]. As a first new application, we present the helicity amplitudes for the process $u^*g \rightarrow ug$. The graphs that have to be taken into account are depicted in Fig. 2. We present the helicity amplitudes with all momenta incoming, *i.e.* for the process

$$0 \rightarrow g(p_1)g(p_2)u(p_u)\bar{u}^*(p_{\bar{u}} + k_T), \quad (20)$$

and we denote

$$p_{\bar{u}} = -x_1\ell_1, \quad k_T = -k_{1\perp}, \quad |k_T| = \sqrt{-k_{1\perp}^2}. \quad (21)$$

The amplitude can be decomposed into two color structures following

$$\mathcal{M}_{ju, j_{\bar{u}}}^{a_1, a_2}(1, 2, u, \bar{u}) = 2ig_S^2 [(T^{a_1} T^{a_2})_{j_u, j_{\bar{u}}} \mathcal{A}(1, 2, u, \bar{u}) + (T^{a_2} T^{a_1})_{j_u, j_{\bar{u}}} \mathcal{A}(2, 1, u, \bar{u})], \quad (22)$$

where the generators of the color group are normalized such that $\text{Tr}\{T^a T^b\} = \frac{1}{2}\delta^{ab}$. The non-zero helicity amplitudes ordered with respect to the gluons are then given by

$$\mathcal{A}(1^+, 2^-, u^+, \bar{u}^+) = -\frac{[\bar{u}|k_T|1\rangle}{|k_T|\langle\bar{u}|1\rangle} \frac{\langle\bar{u}|1\rangle^3\langle u|1\rangle}{\langle u|1\rangle\langle 12\rangle\langle 2\bar{u}\rangle\langle\bar{u}u\rangle}, \quad (23)$$

$$\mathcal{A}(1^-, 2^+, u^+, \bar{u}^+) = -\frac{[\bar{u}|k_T|2\rangle}{|k_T|\langle\bar{u}|2\rangle} \frac{\langle\bar{u}|2\rangle^3\langle u|2\rangle}{\langle u|1\rangle\langle 12\rangle\langle 2\bar{u}\rangle\langle\bar{u}u\rangle}, \quad (24)$$

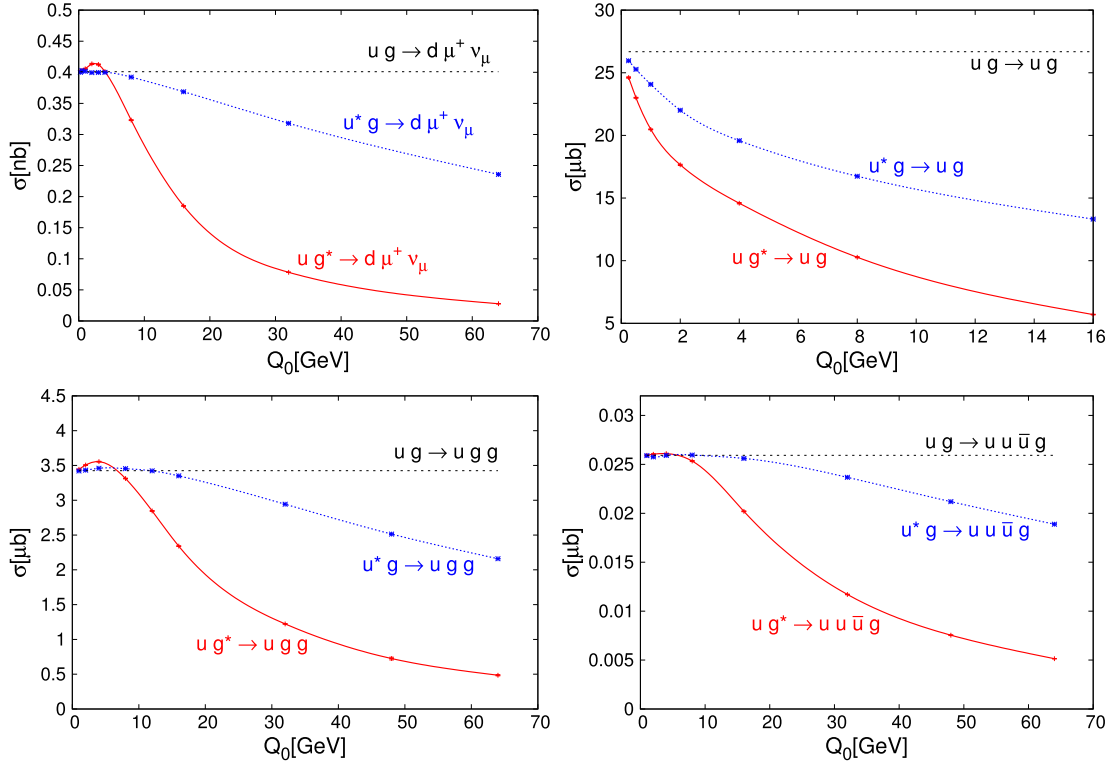


Fig. 3. The cross section of various processes as function of the scale Q_0 in the toy model unintegrated pdf of Eq. (31). The on-shell process does not depend on this scale, and its value corresponds to $Q_0 = 0$. The other curves in each plot correspond to the case of an off-shell initial-state gluon and an off-shell initial-state quark.

$$\mathcal{A}(1^+, 2^-, u^-, \bar{u}^-) = \frac{\langle \bar{u} | k_T | 1 \rangle}{|k_T| \langle \bar{u} | 1 \rangle} \frac{[\bar{u} 1]^3 [u 1]}{[u 1][12][2\bar{u}][\bar{u} u]}, \quad (25)$$

$$\mathcal{A}(1^-, 2^+, u^-, \bar{u}^-) = \frac{\langle \bar{u} | k_T | 2 \rangle}{|k_T| \langle \bar{u} | 2 \rangle} \frac{[\bar{u} 2]^3 [u 2]}{[u 1][12][2\bar{u}][\bar{u} u]}, \quad (26)$$

$$\mathcal{A}(1^+, 2^+, u^-, \bar{u}^-) = -|k_T| \frac{\langle \bar{u} u \rangle^3}{\langle u 1 \rangle \langle 12 \rangle \langle 2\bar{u} \rangle \langle \bar{u} u \rangle}, \quad (27)$$

$$\mathcal{A}(1^-, 2^-, u^+, \bar{u}^+) = |k_T| \frac{[\bar{u} u]^3}{[u 1][12][2\bar{u}][\bar{u} u]}. \quad (28)$$

In [19] it was shown that

$$\left| \frac{[\bar{u} | k_T | 1]}{|k_T| \langle \bar{u} | 1 \rangle} \right| = 1, \quad (29)$$

so we see that the first four amplitudes are, in terms of the four on-shell momenta, identical to the well-known collinear amplitudes [30], apart from a phase factor. Notice that also in the color off-diagonal terms in the squared amplitude, e.g. in $\mathcal{A}(1^+, 2^-, u^+, \bar{u}^+) \mathcal{A}(2^-, 1^+, u^+, \bar{u}^+)^*$, the product of the phase factors is 1, so for the first four helicity configurations, the squared matrix element is given just by the collinear expression evaluated with the on-shell momenta $p_1, p_2, p_u, p_{\bar{u}}$. This seems counter-intuitive, since these momenta do not satisfy momentum conservation. Indeed, a matrix element is *a priori* not unambiguously defined for a set of external momenta that do not satisfy momentum conservation, but a particular explicit expression for that matrix element in terms of the external momenta may be perfectly well defined.

A difference, finally comes with the last two helicity amplitudes, which, contrary to the collinear case, are not identical to zero, but are proportional to $|k_T|$.

The presented prescription to calculate amplitudes with off-shell initial-state quarks has been implemented into a numerical

program, and as a second application, we present cross sections for the processes

$$\begin{aligned} ug \rightarrow d\mu^+ \nu_\mu, \quad u^*g \rightarrow d\mu^+ \nu_\mu, \quad ug^* \rightarrow d\mu^+ \nu_\mu, \\ ug \rightarrow ug, \quad u^*g \rightarrow ug, \quad ug^* \rightarrow ug, \\ ug \rightarrow ugg, \quad u^*g \rightarrow ugg, \quad ug^* \rightarrow ugg, \\ ug \rightarrow uu\bar{u}g, \quad u^*g \rightarrow uu\bar{u}g, \quad ug^* \rightarrow uu\bar{u}g \end{aligned} \quad (30)$$

calculated with the help of a toy model unintegrated pdf closely following [20], namely

$$F(x, k_\perp) = f_a(x, \mu) \frac{\theta(\mu^2 - k_\perp^2)}{Q_0^2 g(x)} \exp\left(-\frac{k_\perp^2}{2Q_0^2 x g(x)}\right). \quad (31)$$

The index a indicates the nature of the off-shell parton, and k_\perp now denotes a two-dimensional transverse vector and not its four-dimensional embedding in Minkowski space. Eq. (31) is to be understood as a tool to study the off-shell matrix elements, in particular their collinear limits. Q_0 determines the typical scale of the transverse momentum components, and for small values the pdf reduces to the collinear pdf

$$\lim_{Q_0 \rightarrow 0} \int \frac{d^2 k_\perp}{2\pi} F(x, k_\perp) = x f_a(x, \mu). \quad (32)$$

The aim of the exercise is to see the difference in behavior between the matrix elements for the off-shell quark and the off-shell gluon. Therefore, we use the same function $g(x)$ for both types of partons, namely the collinear gluon pdf.

Results are presented in Fig. 3. Depicted are cross sections as function of the scale Q_0 . The center-of-mass energy is 14 TeV, and the phase space cuts are $p_T > 20$ GeV and $|y| < 2.8$ for all final-state particles. Also, all pairs of final-state particles have $\Delta R > 0.4$, except in the first process. The collinear pdfs are from

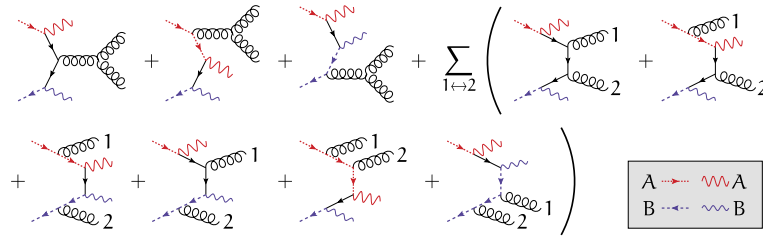


Fig. 4. All graphs contributing to the process $u^* \bar{u}^* \rightarrow gg$ via the embedding $q_A \bar{q}_B \rightarrow \gamma_A \gamma_B gg$.

CTEQ6L1 [31]. The values of the couplings and masses are the same as in [20], and also the scale μ is fixed to the Z -mass again for simplicity.

The straight lines in each of the plots correspond to the collinear case, that is to $Q_0 = 0$. Since the unintegrated pdf is merely a toy model, one should be careful in drawing conclusions from the other curves. It is, however, clear that the matrix elements for the off-shell quark behave very differently from the matrix elements for the off-shell gluon for increasing Q_0 , that is for increasing values of the virtuality of the off-shell parton.

4. Summary

We presented a prescription to calculate manifestly gauge invariant tree-level scattering amplitudes for arbitrary scattering processes with off-shell initial-state quarks within the kinematics of high-energy scattering. Furthermore, we derived explicit expressions for the helicity amplitudes of the process $u^* g \rightarrow ug$, and studied the difference in behavior of the matrix elements between processes $u^* g \rightarrow uX$ and $ug^* \rightarrow uX$ for a number of sets of final-state particles. We see that the matrix elements for off-shell gluons suppress the cross section stronger for increasing values of the transverse momentum than the matrix elements for off-shell quarks.

Acknowledgements

The authors would like to thank P. Kotko for useful discussions and comments. This work was partially supported by HOMING PLUS/2010-2/6: “Matrix Elements and Exclusive Parton Densities for Large Hadron Collider”.

Appendix A. Reproduction of existing results

We compare our approach with the existing results for the processes

$$u^* \bar{u}^* \rightarrow gg, \quad (33)$$

$$u^* g^* \rightarrow ug. \quad (34)$$

The existing results can be found in [23], where they were calculated following the effective action approach of [21].

A.1. $u^* \bar{u}^* \rightarrow gg$

The existing result can be found in Eq. (29) and Eq. (21) of [23]. The graphs contributing to the embedding

$$q_A(k_1) \bar{q}_B(k_2) \rightarrow \gamma_A \gamma_B g(p_1, a, \mu) g(p_2, b, \nu) \quad (35)$$

in our approach are depicted in Fig. 4. Using the relation

$$-ig_S^2 T^c f^{cab} = (-igs)(-igs)[T^a, T^b] \quad (36)$$

we split the graphs with the 3-gluon vertex into two parts. The amplitude can, before contraction with the polarization vectors of the external gluons, be written as

$$\mathcal{M}_{-,-}^{ab,\mu\nu} = \sqrt{\frac{x_1 x_2 k_1^2 k_2^2}{4}} (-igs)^2 \langle \ell_2 | [C^{\mu\nu}(p_1, p_2) T^a T^b + C^{\nu\mu}(p_2, p_1) T^b T^a] | \ell_1 \rangle, \quad (37)$$

and we only need to calculate $C^{\nu\mu}(p_2, p_1)$. The spinors $|\ell_1\rangle, \langle\ell_2|$ are those assigned to the external auxiliary quarks q_A and \bar{q}_B respectively and both have negative helicity. The mixed-helicity cases vanish, and the positive helicity case will be dealt with later. According to our prescription, the polarization vectors for the auxiliary photons are then given by

$$\varepsilon_A^\mu = \frac{\langle \ell_1 | \gamma^\mu | \ell_2 \rangle}{\sqrt{2} \langle \ell_1 | \ell_2 \rangle}, \quad \varepsilon_B^\mu = \frac{\langle \ell_1 | \gamma^\mu | \ell_2 \rangle}{\sqrt{2} \langle \ell_1 | \ell_2 \rangle}. \quad (38)$$

Remember that for the B -photon ℓ_1 and ℓ_2 switch role. The 3-gluon vertex with momentum conservation imposed and a propagator denominator included we denote by

$$V^{\sigma\mu\nu}(p_1, p_2) = \frac{1}{(p_1 + p_2)^2} [(p_1 - p_2)^\sigma \eta^{\mu\nu} + (2p_2 + p_1)^\mu \eta^{\nu\sigma} - (2p_1 + p_2)^\nu \eta^{\mu\sigma}]. \quad (39)$$

The graphs contribute, in the Feynman gauge, to $C^{\nu\mu}(p_2, p_1)$ as follows:

$$C^{\nu\mu}(p_2, p_1) = (-i\not{p}_B) \frac{i}{-k_2} (-i\gamma_\sigma) V^{\sigma\nu\mu}(p_2, p_1) \frac{i}{k_1} (-i\not{p}_A) \quad (40)$$

$$+ (-i\not{p}_B) \frac{i}{-k_2} (-i\not{p}_A) \frac{i\not{\ell}_1}{2\ell_1 \cdot (k_1 - p_1 - p_2)} (-i\gamma_\sigma) \times V^{\sigma\nu\mu}(p_2, p_1) \quad (41)$$

$$+ (-i\gamma_\sigma) V^{\sigma\nu\mu}(p_2, p_1) \frac{i\not{\ell}_2}{2\ell_2 \cdot (-k_2 + p_1 + p_2)} (-i\not{p}_B) \times \frac{i}{k_1} (-i\not{p}_A) \quad (42)$$

$$+ (-i\not{p}_B) \frac{i}{-k_2} \gamma^\nu \frac{i}{k_1 - \not{p}_1} \gamma^\mu \frac{i}{k_1} (-i\not{p}_A) \quad (43)$$

$$+ (-i\not{p}_B) \frac{i}{-k_2} \gamma^\nu \frac{i}{k_1 - \not{p}_1} (-i\not{p}_A) \frac{i\not{\ell}_1}{2\ell_1 \cdot (k_1 - p_1)} \gamma^\mu \quad (44)$$

$$+ \gamma^\nu \frac{i\not{\ell}_2}{2\ell_2 \cdot (-k_2 + p_2)} (-i\not{p}_B) \frac{i}{k_1 - \not{p}_1} (-i\not{p}_A) \times \frac{i\not{\ell}_1}{2\ell_1 \cdot (k_1 - p_1)} \gamma^\mu \quad (45)$$

$$+ \gamma^\nu \frac{i\not{\ell}_2}{2\ell_2 \cdot (-k_2 + p_2)} (-i\not{p}_B) \frac{i}{k_1 - \not{p}_1} \gamma^\mu \frac{i}{k_1} (-i\not{p}_A) \quad (46)$$

$$\begin{aligned}
 &+ (-i\phi_B) \frac{i}{-k_2} (-i\phi_A) \frac{i\ell_1}{2\ell_1 \cdot (k_1 - p_1 - p_2)} \gamma^\nu \\
 &\times \frac{i\ell_1}{2\ell_1 \cdot (k_1 - p_1)} \gamma^\mu \quad (47)
 \end{aligned}$$

$$\begin{aligned}
 &+ \gamma^\nu \frac{i\ell_2}{2\ell_2 \cdot (-k_2 + p_2)} \gamma^\mu \frac{i\ell_2}{2\ell_2 \cdot (-k_2 + p_1 + p_2)} (-i\phi_B) \\
 &\times \frac{i}{k_1} (-i\phi_A). \quad (48)
 \end{aligned}$$

After some re-arrangements of terms and using the fact that $\ell_1 \cdot k_1 = \ell_2 \cdot k_2 = 0$, and therefore also

$$\begin{aligned}
 \ell_1 \cdot (p_1 + p_2) &= \ell_1 \cdot (k_1 + k_2) = \ell_1 \cdot k_2, \\
 \ell_2 \cdot (p_1 + p_2) &= \ell_2 \cdot (k_1 + k_2) = \ell_2 \cdot k_1, \quad (49)
 \end{aligned}$$

we find

$$\begin{aligned}
 &-iC^{\nu\mu}(p_2, p_1) \\
 &= \left(\phi_B \frac{1}{k_2} \gamma_\sigma \frac{1}{k_1} \phi_A - \phi_B \frac{1}{k_2} \phi_A \frac{\ell_1}{2\ell_1 \cdot k_2} \gamma_\sigma \right. \\
 &\quad \left. - \gamma_\sigma \frac{\ell_2}{2\ell_2 \cdot k_1} \phi_B \frac{1}{k_1} \phi_A \right) V^{\sigma\nu\mu}(p_2, p_1) \\
 &+ \left(\phi_B \frac{1}{k_2} \gamma^\nu - \gamma^\nu \frac{\ell_2}{2\ell_2 \cdot p_2} \phi_B \right) \frac{1}{p_1 - k_1} \\
 &\times \left(\gamma^\mu \frac{1}{k_1} \phi_A - \phi_A \frac{\ell_1}{2\ell_1 \cdot p_1} \gamma^\mu \right) \\
 &- \phi_B \frac{1}{k_2} \phi_A \frac{\ell_1}{2\ell_1 \cdot k_2} \gamma^\nu \frac{\ell_1}{2\ell_1 \cdot p_1} \gamma^\mu \\
 &+ \gamma^\nu \frac{\ell_2}{2\ell_2 \cdot p_2} \gamma^\mu \frac{\ell_2}{2\ell_2 \cdot k_1} \phi_B \frac{1}{k_1} \phi_A. \quad (50)
 \end{aligned}$$

It turns out to be convenient to insert $1 = k_1/k_1$ and $1 = k_2/k_2$ at some points:

$$\begin{aligned}
 &-iC^{\nu\mu}(p_2, p_1) \\
 &= \left(\phi_B \frac{1}{k_2} \gamma_\sigma \frac{1}{k_1} \phi_A - \phi_B \frac{1}{k_2} k_1 \frac{1}{k_1} \phi_A \frac{\ell_1}{2\ell_1 \cdot k_2} \gamma_\sigma \right. \\
 &\quad \left. - \gamma_\sigma \frac{\ell_2}{2\ell_2 \cdot k_1} \phi_B \frac{1}{k_2} k_2 \frac{1}{k_1} \phi_A \right) V^{\sigma\nu\mu}(p_2, p_1) \\
 &+ \left(\phi_B \frac{1}{k_2} \gamma^\nu - \gamma^\nu \frac{\ell_2}{2\ell_2 \cdot p_2} \phi_B \frac{1}{k_2} k_2 \right) \frac{1}{p_1 - k_1} \\
 &\times \left(\gamma^\mu \frac{1}{k_1} \phi_A - k_1 \frac{1}{k_1} \phi_A \frac{\ell_1}{2\ell_1 \cdot p_1} \gamma^\mu \right) \\
 &- \phi_B \frac{1}{k_2} k_1 \frac{1}{k_1} \phi_A \frac{\ell_1}{2\ell_1 \cdot k_2} \gamma^\nu \frac{\ell_1}{2\ell_1 \cdot p_1} \gamma^\mu \\
 &+ \gamma^\nu \frac{\ell_2}{2\ell_2 \cdot p_2} \gamma^\mu \frac{\ell_2}{2\ell_2 \cdot k_1} \phi_B \frac{1}{k_2} k_2 \frac{1}{k_1} \phi_A. \quad (51)
 \end{aligned}$$

Now, we apply the fact that

$$\begin{aligned}
 \ell_1 &= |\ell_1\rangle[\ell_1] + |\ell_1\rangle\langle\ell_1|, & \ell_3 &= |\ell_2\rangle[\ell_1] + |\ell_1\rangle\langle\ell_2|, \\
 \ell_2 &= |\ell_2\rangle[\ell_2] + |\ell_2\rangle\langle\ell_2|, & \ell_4 &= |\ell_1\rangle[\ell_2] + |\ell_2\rangle\langle\ell_1|
 \end{aligned} \quad (52)$$

and

$$\phi_A = \frac{\sqrt{2}}{[\ell_1|\ell_2]} \ell_4, \quad \phi_B = \frac{\sqrt{2}}{\langle\ell_1|\ell_2\rangle} \ell_4 \quad (53)$$

and the general relations

$$\begin{aligned}
 [p|p] &= \langle p|p\rangle = 0, & [q|p] &= [q|p] = 0, \\
 \langle p|\gamma^\mu|q\rangle &= [p|\gamma^\mu|q] = 0, \\
 [p|q] &= -[q|p], & \langle p|q\rangle &= -\langle q|p\rangle, & \langle p|\gamma^\mu|q\rangle &= [q|\gamma^\mu|p], \\
 \langle p|\gamma^\mu|p\rangle &= 2p^\mu, & [p|q]\langle q|p\rangle &= 2p \cdot q. \quad (54)
 \end{aligned}$$

We get

$$\langle\ell_2|\phi_B = -\sqrt{2}|\ell_2\rangle, \quad (55)$$

$$\langle\ell_2|\gamma^\sigma \frac{\ell_2}{2\ell_2 \cdot k_1} \phi_B = -\sqrt{2} \frac{\ell_2^\sigma}{\ell_2 \cdot k_1} |\ell_2\rangle, \quad (56)$$

$$\langle\ell_2|\gamma^\nu \frac{\ell_2}{2\ell_2 \cdot p_2} \gamma^\mu \frac{\ell_2}{2\ell_2 \cdot k_1} \phi_B = -\sqrt{2} \frac{\ell_2^\nu}{\ell_2 \cdot p_2} \frac{\ell_2^\mu}{\ell_2 \cdot k_1} |\ell_2\rangle \quad (57)$$

and likewise

$$\phi_A|\ell_1] = -\sqrt{2}|\ell_1], \quad (58)$$

$$\phi_A \frac{\ell_1}{2\ell_1 \cdot k_2} \gamma^\sigma |\ell_1] = -\sqrt{2} \frac{\ell_1^\sigma}{\ell_1 \cdot k_2} |\ell_1], \quad (59)$$

$$\phi_A \frac{\ell_1}{2\ell_1 \cdot k_2} \gamma^\nu \frac{\ell_1}{2\ell_1 \cdot p_1} \gamma^\mu |\ell_1] = -\sqrt{2} \frac{\ell_1^\nu}{\ell_1 \cdot k_2} \frac{\ell_1^\mu}{\ell_1 \cdot p_1} |\ell_1]. \quad (60)$$

Inserting these relations, we get

$$\langle\ell_2|C^{\nu\mu}(p_2, p_1)|\ell_1] = 2i[\ell_2| \frac{1}{k_2} D^{\nu\mu}(p_2, p_1) \frac{1}{k_1} |\ell_1], \quad (61)$$

where

$$\begin{aligned}
 D^{\nu\mu}(p_2, p_1) &= \left(\gamma_\sigma - k_1 \frac{\ell_{1\sigma}}{\ell_1 \cdot k_2} - k_2 \frac{\ell_{2\sigma}}{\ell_2 \cdot k_1} \right) V^{\sigma\nu\mu}(p_2, p_1) \\
 &+ \left(\gamma^\nu - k_2 \frac{\ell_2^\nu}{\ell_2 \cdot p_2} \right) \frac{1}{p_1 - k_1} \left(\gamma^\mu - k_1 \frac{\ell_1^\mu}{\ell_1 \cdot p_1} \right) \\
 &- k_1 \frac{\ell_1^\nu}{\ell_1 \cdot k_2} \frac{\ell_1^\mu}{\ell_1 \cdot p_1} + k_2 \frac{\ell_2^\nu}{\ell_2 \cdot k_1} \frac{\ell_2^\mu}{\ell_2 \cdot p_2}. \quad (62)
 \end{aligned}$$

One can now already recognize the terms from Eq. (21) of [23], with the identifications

$$\ell_1 \leftrightarrow n^-, \quad \ell_2 \leftrightarrow n^+, \quad (63)$$

$$\gamma^\mu - k_1 \frac{\ell_1^\mu}{\ell_1 \cdot p_1} \leftrightarrow \gamma^{(-)\mu}(k_1, -p_1),$$

$$\gamma^\nu - k_2 \frac{\ell_2^\nu}{\ell_2 \cdot p_2} \leftrightarrow \gamma^{(+)\nu}(k_2, -p_2), \quad (64)$$

$$\gamma_\sigma - k_1 \frac{\ell_{1\sigma}}{\ell_1 \cdot k_2} - k_2 \frac{\ell_{2\sigma}}{\ell_2 \cdot k_1} \leftrightarrow \gamma_\sigma^{(+,-)}(k_1, k_2). \quad (65)$$

More precisely, and remembering that $p_1 - k_1 = k_2 - p_2$, we find

$$\begin{aligned}
 C_{Q\bar{Q}}^{g\bar{g},ab,\mu\nu}(k_1, k_2, p_1, p_2) \\
 = g_S^2 [D^{\mu\nu}(p_1, p_2) T^a T^b + D^{\nu\mu}(p_2, p_1) T^b T^a]. \quad (66)
 \end{aligned}$$

So we arrived at

$$\mathcal{M}_{-,-}^{ab,\mu\nu} = -i\sqrt{x_1 x_2 k_1^2 k_2^2} [\ell_2| \frac{1}{k_2} C_{Q\bar{Q}}^{g\bar{g},ab,\mu\nu} \frac{1}{k_1} |\ell_1]. \quad (67)$$

Writing k_1 and k_2 in terms of $\ell_{1,2,3,4}$ and using $[\ell_2|\ell_2] = [\ell_2|\ell_4] = \ell_1|\ell_1] = \ell_4|\ell_1] = 0$, we have

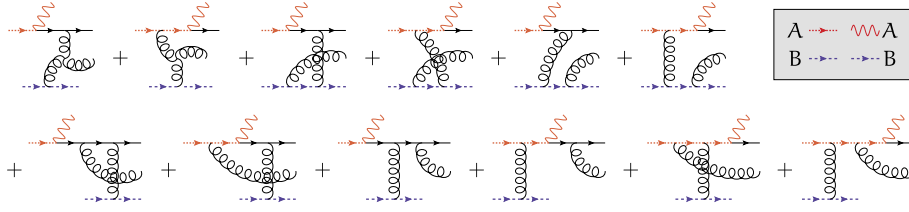


Fig. 5. All graphs contributing to the process $u^*g^* \rightarrow ug$ via the embedding $q_A q_B \rightarrow \gamma_A q_B u g$.

$$\begin{aligned}
 \langle \ell_2 | \frac{1}{k_2} &= \frac{1}{k_2^2} \langle \ell_2 | k_2 = \frac{1}{k_2^2} \langle \ell_2 | \ell_3 \frac{-k_{2\perp} \cdot \ell_4}{\ell_1 \cdot \ell_2} \\
 &= \frac{1}{k_2^2} \langle \ell_2 | \ell_1 \rangle \langle \ell_2 | \frac{-k_{2\perp} \cdot \ell_4}{\ell_1 \cdot \ell_2}, \quad (68)
 \end{aligned}$$

$$\begin{aligned}
 \frac{1}{k_1} | \ell_1 \rangle &= \frac{1}{k_1^2} k_1 | \ell_1 \rangle = \frac{1}{k_1^2} \frac{-k_{1\perp} \cdot \ell_4}{\ell_1 \cdot \ell_2} \ell_3 | \ell_1 \rangle \\
 &= \frac{1}{k_1^2} \frac{-k_{1\perp} \cdot \ell_4}{\ell_1 \cdot \ell_2} | \ell_1 \rangle \langle \ell_2 | \ell_1 \rangle. \quad (69)
 \end{aligned}$$

Using furthermore that $\langle \ell_2 | \ell_1 \rangle \langle \ell_2 | \ell_1 \rangle = -2\ell_1 \cdot \ell_2$ and $\sqrt{x_2} \langle \ell_2 | = \langle x_2 \ell_2 |$ and $\sqrt{x_1} | \ell_1 \rangle = | x_1 \ell_1 \rangle$ we find

$$\mathcal{M}_{-,-}^{ab,\mu\nu} = i \sqrt{\frac{1}{k_1^2 k_2^2}} \frac{2k_{1\perp} \cdot \ell_4 k_{2\perp} \cdot \ell_4}{\ell_1 \cdot \ell_2} \langle x_2 \ell_2 | C_{Q\bar{Q}}^{gg,ab,\mu\nu} | x_1 \ell_1 \rangle. \quad (70)$$

And thus we established the equality with Eq. (29) of [23] up to a phase factor, as is clear from Eq. (15). The reader may convince themselves that

$$\mathcal{M}_{+,+}^{ab,\mu\nu} = i \sqrt{\frac{1}{k_1^2 k_2^2}} \frac{2k_{1\perp} \cdot \ell_3 k_{2\perp} \cdot \ell_3}{\ell_1 \cdot \ell_2} [x_2 \ell_2 | C_{Q\bar{Q}}^{gg,ab,\mu\nu} | x_1 \ell_1 \rangle. \quad (71)$$

A.2. $u^*g^* \rightarrow ug$

The existing result can be found in Eq. (24) and Eq. (16) of [23]. The graphs contributing to the embedding

$$q_A(k_1) q_B(k_2) \rightarrow \gamma_A q_B u(p_1) g(p_2, \mu, b)$$

are depicted in Fig. 5. Rather than going through the whole calculation in all detail, we identify which graphs contribute to which terms in Eq. (16) of [23].

First of all, we recognize that all graphs except the last two can be paired according to the occurrence of the combination

$$\begin{aligned}
 k_1 \cdots \begin{array}{c} \circ \\ \circ \\ \circ \end{array} \cdots p_1 + k_1 \cdots \begin{array}{c} \circ \\ \circ \\ \circ \end{array} \cdots p_1 \\
 \begin{array}{c} \circ \\ \circ \\ \circ \end{array} c, \sigma & \quad \begin{array}{c} \circ \\ \circ \\ \circ \end{array} c, \sigma \\
 &= (-i\gamma^\sigma T^c) \frac{i}{k_1} (-i\cancel{\not{A}}) | \ell_1 \rangle + (-i\cancel{\not{A}}) \frac{i\cancel{\not{A}}}{2\ell_1 \cdot p_1} (-i\gamma^\sigma T^c) | \ell_1 \rangle \\
 &= \sqrt{2}i \left(\gamma^\sigma \frac{1}{k_1} + \frac{\cancel{\not{A}}^\sigma}{\ell_1 \cdot p_1} \right) | \ell_1 \rangle T^c \\
 &= \sqrt{2}i \gamma^{(-)\sigma}(k_1, p_1) \frac{1}{k_1} | \ell_1 \rangle T^c \quad (72)
 \end{aligned}$$

with the *induced vertex*

$$\gamma^{(-)\sigma}(k_1, p_1) = \gamma^\sigma + k_1 \frac{\cancel{\not{A}}^\sigma}{\ell_1 \cdot p_1} = \gamma^\sigma + k_1 \frac{\cancel{\not{A}}^\sigma}{\ell_1 \cdot (p_1 - k_1)}. \quad (73)$$

The factor $k_1^{-1} | \ell_1 \rangle$ evaluates further following Eq. (69). Furthermore, we recognize in the last four graphs of the first line of Fig. 5 another *induced vertex*

$$\begin{aligned}
 \begin{array}{c} c, \sigma & b, \mu, p_2 \\ \circ & \circ \\ \circ & \circ \\ \circ & \circ \end{array} & + \begin{array}{c} c, \sigma & b, \mu, p_2 \\ \circ & \circ \\ \circ & \circ \\ \circ & \circ \end{array} \\
 k_2 \cdots \begin{array}{c} \circ \\ \circ \\ \circ \end{array} \cdots & \quad k_2 \cdots \begin{array}{c} \circ \\ \circ \\ \circ \end{array} \cdots \\
 &= \langle \ell_2 | (-i\gamma^\mu T^b) \frac{i\cancel{\not{A}}}{2\ell_2 \cdot p_2} (-i\gamma^\sigma T^c) | \ell_2 \rangle \\
 &\quad + \langle \ell_2 | (-i\gamma^\sigma T^c) \frac{i\cancel{\not{A}}}{2\ell_2 \cdot (k_2 - p_2)} (-i\gamma^\mu T^b) | \ell_2 \rangle \\
 &= -2i \frac{\cancel{\not{A}}^\mu \cancel{\not{A}}^\sigma}{\ell_2 \cdot p_2} [T^b, T^c] = 2 \frac{\cancel{\not{A}}^\mu \cancel{\not{A}}^\sigma}{\ell_2 \cdot p_2} f^{abc} T^a. \quad (74)
 \end{aligned}$$

So all graphs on the first line have the same color factor, and we may remove the T^a coming from our rules [29] from all graphs. The color index a then indicates the off-shell initial-state gluon. It is then straightforward to see that the whole first line of Fig. 5 contributes the terms

$$\begin{aligned}
 \frac{1}{k_2^2} \gamma^{(-)\sigma}(k_1, p_1) \frac{1}{(k_1 - p_1)^2} \\
 \times \left(\gamma^{\mu\nu\sigma}(p_2, -k_2) \ell_{2\nu} + k_2^2 \frac{\cancel{\not{A}}^\mu \cancel{\not{A}}^\sigma}{\ell_2 \cdot p_2} \right) [T^a, T^b] \quad (75)
 \end{aligned}$$

from the expression of [23]. The extra factor $\sqrt{k_2^-}$ that has to be provided according to our rules reduces the factor k_2^2 in the denominator to $\sqrt{k_2^-}$. Realize that $\ell_{1,2}$ are dimensionful contrary to n^\pm . This difference manifests itself in the overall factor q_2^- in the expression of [23] which does not occur here. This factor also contains the x_2 that has to be provided separately according to our rules.

One can also easily recognize that the first two graphs on the second line of Fig. 5 contribute

$$-\frac{1}{k_2^2} \cancel{\not{A}} \frac{1}{k_1 - p_2} \gamma^{(-)\mu}(k_1, -p_2) T^a T^b, \quad (76)$$

and the third and the fourth graphs contribute

$$-\frac{1}{k_2^2} \gamma^\mu \frac{1}{k_1 + k_2} \gamma^{(-)\sigma}(k_1, k_2) \ell_{2\sigma} T^b T^a. \quad (77)$$

The last two graphs, finally, can easily be seen to contribute

$$\frac{1}{k_2^2} \frac{2k_1 \cancel{\not{A}}^\mu}{\ell_1 \cdot p_1} \left(\frac{T^a T^b}{\ell_1 \cdot p_2} - \frac{T^b T^a}{\ell_1 \cdot k_2} \right). \quad (78)$$

The factor k_1 facilitates a compensating k_1^{-1} necessary to write the contribution of the graphs such that they contain $k_1^{-1} | \ell_1 \rangle$ following Eq. (72).

References

- [1] R.K. Ellis, H. Georgi, M. Machacek, H.D. Politzer, G.G. Ross, *Perturbation theory and the parton model in QCD*, Nucl. Phys. B 152 (1979) 285.
- [2] P. Mulders, T. Rogers, *Gauge links, TMD-factorization, and TMD-factorization breaking*, arXiv:1102.4569.

- [3] L. Gribov, E. Levin, M. Ryskin, Semihard processes in QCD, *Phys. Rep.* 100 (1983) 1–150.
- [4] S. Catani, M. Ciafaloni, F. Hautmann, High-energy factorization and small x heavy flavor production, *Nucl. Phys. B* 366 (1991) 135–188.
- [5] E. Kuraev, L. Lipatov, V.S. Fadin, Multi-reggeon processes in the Yang–Mills theory, *Sov. Phys. JETP* 44 (1976) 443–450.
- [6] E. Kuraev, L. Lipatov, V.S. Fadin, The pomeron singularity in nonabelian gauge theories, *Sov. Phys. JETP* 45 (1977) 199–204.
- [7] I. Balitsky, L. Lipatov, The pomeron singularity in quantum chromodynamics, *Sov. J. Nucl. Phys.* 28 (1978) 822–829.
- [8] M. Ciafaloni, Coherence effects in initial jets at small q^2/s , *Nucl. Phys. B* 296 (1988) 49.
- [9] S. Catani, F. Fiorani, G. Marchesini, Small x behavior of initial state radiation in perturbative QCD, *Nucl. Phys. B* 336 (1990) 18.
- [10] S. Catani, F. Fiorani, G. Marchesini, QCD coherence in initial state radiation, *Phys. Lett. B* 234 (1990) 339.
- [11] I. Balitsky, Operator expansion for high-energy scattering, *Nucl. Phys. B* 463 (1996) 99–160, arXiv:hep-ph/9509348.
- [12] Y.V. Kovchegov, Small- x F_2 structure function of a nucleus including multiple pomeron exchanges, *Phys. Rev. D* 60 (1999) 034008, arXiv:hep-ph/9901281.
- [13] Y.V. Kovchegov, Unitarization of the BFKL pomeron on a nucleus, *Phys. Rev. D* 61 (2000) 074018, arXiv:hep-ph/9905214.
- [14] K. Kutak, K. Golec-Biernat, S. Jadach, M. Skrzypek, Nonlinear equation for coherent gluon emission, *JHEP* 1202 (2012) 117, arXiv:1111.6928.
- [15] K. Kutak, Nonlinear extension of the CCFM equation, arXiv:1206.1223.
- [16] K. Kutak, Resummation in nonlinear equation for high energy factorisable gluon density and its extension to include coherence, arXiv:1206.5757.
- [17] L. Lipatov, Gauge invariant effective action for high-energy processes in QCD, *Nucl. Phys. B* 452 (1995) 369–400, arXiv:hep-ph/9502308.
- [18] E. Antonov, L. Lipatov, E. Kuraev, I. Cherednikov, Feynman rules for effective Regge action, *Nucl. Phys. B* 721 (2005) 111–135, arXiv:hep-ph/0411185.
- [19] A. van Hameren, P. Kotko, K. Kutak, Multi-gluon helicity amplitudes with one off-shell leg within high energy factorization, *J. High Energy Phys.* 1212 (2012) 029, arXiv:1207.3332.
- [20] A. van Hameren, P. Kotko, K. Kutak, Helicity amplitudes for high-energy scattering, *J. High Energy Phys.* 1301 (2013) 078, arXiv:1211.0961.
- [21] L. Lipatov, M. Vyazovsky, Quasi-multi-Regge processes with a quark exchange in the t channel, *Nucl. Phys. B* 597 (2001) 399–409, arXiv:hep-ph/0009340.
- [22] A. Bogdan, V. Fadin, A proof of the reggeized form of amplitudes with quark exchanges, *Nucl. Phys. B* 740 (2006) 36–57, arXiv:hep-ph/0601117.
- [23] M. Nefedov, V. Saleev, A.V. Shipilova, Dijet azimuthal decorrelations at the LHC in the parton Reggeization approach, *Phys. Rev. D* 87 (2013) 094030, arXiv:1304.3549.
- [24] F. Hautmann, M. Hentschinski, H. Jung, Forward Z-boson production and the unintegrated sea quark density, *Nucl. Phys. B* 865 (2012) 54–66, arXiv:1205.1759.
- [25] F. Hautmann, M. Hentschinski, H. Jung, TMD PDFs: A Monte Carlo implementation for the sea quark distribution, arXiv:1205.6358.
- [26] V. Saleev, Deep inelastic scattering and prompt photon production within the framework of quark Reggeization hypothesis, *Phys. Rev. D* 78 (2008) 034033, arXiv:0807.1587.
- [27] B. Kniesl, A. Shipilova, V. Saleev, Open charm production at high energies and the quark Reggeization hypothesis, *Phys. Rev. D* 79 (2009) 034007, arXiv:0812.3376.
- [28] B. Ermolaev, M. Greco, S. Troyan, QCD factorization for forward hadron scattering at high energies, *Eur. Phys. J. C* 72 (2012) 1953, arXiv:1112.1854.
- [29] A. van Hameren, Scattering amplitudes for high-energy factorization, arXiv:1307.1979.
- [30] M.L. Mangano, S.J. Parke, Multiparton amplitudes in gauge theories, *Phys. Rep.* 200 (1991) 301–367, arXiv:hep-th/0509223.
- [31] J. Pumplin, D. Stump, J. Huston, H. Lai, P.M. Nadolsky, et al., New generation of parton distributions with uncertainties from global QCD analysis, *J. High Energy Phys.* 0207 (2002) 012, arXiv:hep-ph/0201195.